

MAD/PH/814  
June 1994

## Evidence for a Hard Pomeron in Perturbative QCD

Hassan N. Chehime and Dieter Zeppenfeld

*Department of Physics, University of Wisconsin, Madison, WI 53706, USA*

### ABSTRACT

The  $t$ -channel exchange of two gluons in a color singlet state represents the lowest order approximation to the Pomeron. This exchange mechanism is thought to also explain the formation of rapidity gaps in dijet events at the Tevatron. At the perturbative level this requires suppressed gluon emission in the rapidity interval between widely separated jets, analogous to color coherence effects in  $t$ -channel photon exchange. By calculating the imaginary part of the two gluon, color singlet exchange amplitude we show how this pattern does emerge for gluon emission at small transverse momenta. At large  $p_T$  the radiation pattern characteristic for color octet single gluon exchange is reproduced.

arXiv:hep-ph/9401244v2 14 Jul 1994

## I. INTRODUCTION

Over the past three decades the Pomeron model has been very successful in describing a wealth of data on hadronic collisions: the total cross section, elastic scattering, and single diffractive scattering [1–4]. As viewed from perturbative QCD the Pomeron may be thought of as the  $t$ -channel exchange of two gluons in a color singlet state [2]. This simple picture, to be called the Low-Nussinov Pomeron in the following, has been refined in subsequent years in terms of reggeized gluon ladders leading to the Lipatov hard Pomeron [3].

One of the defining features of diffractive scattering is the pattern of final state hadrons. In a collider configuration hadronization occurs in narrow cones around the beam directions while the central rapidity region is free of produced hadrons (rapidity gap). The same phenomenon has recently been observed in *hard* scattering events at the Tevatron [5]. The D0 Collaboration has studied a sample of dijet events with jet transverse energies in excess of 30 GeV. In about 0.5% of all events with widely separated jets no sign of hadronic activity is observed between the two jets.

This observation is consistent with predictions for rapidity gap event rates within the Pomeron model [6]. Bjorken estimated the size of the Low-Nussinov Pomeron exchange contribution and found that a fraction  $f \approx 10\%$  of all dijet events should be due to this mechanism. The other factor in his estimate is the “survival probability”  $P_s$ , *i.e.* the probability that the underlying event does not fill the rapidity gap which is present at the parton level. The survival probability is expected to be of order 10% at the Tevatron, with large uncertainties [6,7], leading to a rapidity gap fraction  $fP_s = 0.01$ , as compared to the observation at the 0.005 level.

Both Pomeron and  $t$ -channel photon exchange are believed to lead to rapidity gaps since both scattering processes proceed via the exchange of a  $t$ -channel color singlet object. In the case of  $\gamma$  exchange in forward  $qq \rightarrow qq$  scattering, color coherence [8] between initial and final state gluon radiation is known to lead to an exponentially suppressed gluon emission probability into the rapidity region between the two final state quarks [9]. After hadronization this translates into suppressed hadronic activity between the two quark jets, thus allowing the formation of a rapidity gap. Due to its color singlet structure one expects that the same would occur for the  $t$ -channel exchange of a Pomeron. However, since the Low-Nussinov Pomeron is an extended object with colored constituents, the validity of this analogy is not obvious: gluon radiation may resolve the internal color structure of the Pomeron.

In this paper we investigate the conditions (if any) under which gluon emission between the two final state quarks is suppressed in the Pomeron exchange process. This radiation pattern is necessary for the interpretation of the sizable rate of rapidity gap events observed by D0 since electroweak processes alone, *i.e.*  $t$ -channel  $\gamma$ ,  $Z$  or  $W$  exchange, have too small a cross section to account for the observed rate [10]. We calculate the gluon radiation pattern for the imaginary part of the  $t$ -channel exchange of two gluons in quark-quark scattering. There are practical reasons why we do not attempt a full calculation. The lowest order cross section for gluon radiation in two gluon color singlet exchange is of order  $\alpha_s^5$  and hence the full calculation corresponds to a two-loop evaluation of 3-jet production at hadron colliders, which is clearly beyond the scope of the present work. Instead, we aim at a qualitative understanding of the radiation pattern only. Since the imaginary part of the amplitude is known to dominate over the real part in forward, elastic quark-quark scattering

via Pomeron exchange [11], the imaginary part of the emission process should be sufficient for our purposes.

The gluon radiation pattern for color singlet two-gluon exchange is then compared to the ones obtained for (color singlet)  $\gamma$  exchange and for (color octet) gluon exchange. For the exchange of a Low-Nussinov Pomeron we find that the angular distribution of a single radiated gluon can be described in terms of three components: a QED-like contribution which is consistent with the formation of rapidity gaps, a QCD like term with gluon emission in the backwards direction, and a collinear term which describes  $q \rightarrow g$  splitting and subsequent Pomeron exchange between the gluon and the second quark. For the emission of gluons at low transverse momentum the QED-like component is much larger than the QCD-like one. Since these soft gluons dominate the overall gluon radiation, hadronization will produce a pattern similar to the one expected for  $t$ -channel photon exchange. Therefore Pomeron exchange should indeed lead to the formation of rapidity gaps in hard scattering events. For those willing to extrapolate to low  $|t|$  this finding gives further credence to a QCD explanation also of the soft Pomeron.

The main part of this paper is organized as follows. In Section II we discuss the most general color structure of the  $qQ \rightarrow qQg$  process. Two of the terms in the color decomposition define what we mean by “color singlet exchange in the  $t$ -channel”. We then apply this decomposition to the tree level photon and single gluon exchange processes, which are later needed for comparison, and discuss their radiation patterns. Section III is technical and describes our calculation of the imaginary part of  $qQ \rightarrow qQg$  scattering via two gluon exchange. The resulting radiation pattern is then discussed in Section IV and Section V gives our conclusions.

## II. COLOR STRUCTURE AND TREE LEVEL AMPLITUDES

We start by analyzing the color structure and the resulting gluon radiation patterns for the scattering of two quarks of different flavor at tree level. The amplitudes for single gluon and single photon exchange already exhibit the full color structure of the process  $qQ \rightarrow qQg$  and these results will be needed later for comparison with Pomeron exchange. We thus study the process

$$q(p_1, i_1) Q(p_3, i_3) \longrightarrow q(p_2, i_2) Q(p_4, i_4) g(k, a) , \quad (1)$$

where  $p_n$  and  $k$  denote the quark and gluon momenta and their colors are labeled by  $i_n$  and  $a$ . Scattering involving anti-quarks is related by crossing and we do not consider processes with initial state gluons.

In general, the amplitude of the  $qQ \rightarrow qQg$  process can be written in terms of four orthogonal color tensors, which we denote by  $O_1$ ,  $O_2$ ,  $S_{12}$ , and  $S_{34}$ ,

$$M = O_1 M_1 + O_2 M_2 + S_{12} M_{12} + S_{34} M_{34} . \quad (2)$$

In an  $SU(N)$  gauge theory they are given explicitly by

$$S_{12} = \frac{\lambda_{i_4 i_3}^a}{2} \delta_{i_2 i_1} \quad (3)$$

$$S_{34} = \frac{\lambda_{i_2 i_1}^a}{2} \delta_{i_4 i_3} \quad (4)$$

$$O_1 = \frac{-2}{N} (S_{12} + S_{34}) + \frac{\lambda_{i_2 i_3}^a}{2} \delta_{i_4 i_1} + \frac{\lambda_{i_4 i_1}^a}{2} \delta_{i_2 i_3} \quad (5)$$

$$O_2 = \frac{\lambda_{i_4 i_1}^a}{2} \delta_{i_2 i_3} - \frac{\lambda_{i_2 i_3}^a}{2} \delta_{i_4 i_1} . \quad (6)$$

$S_{12}$  marks the process where the quark  $q$  keeps its color. Similarly,  $S_{34}$  multiplies the amplitude for  $t$ -channel color singlet exchange as viewed from quark  $Q$ . Within QCD,  $O_1$  and  $O_2$  correspond to  $t$ -channel color octet exchange as viewed from either of the two scattering quarks.

Let us first apply this color decomposition to the tree level QED and QCD amplitudes. The five Feynman graphs for the QCD process are shown in Fig. 1. Lumping the momentum and helicity dependence of the individual Feynman diagrams into reduced amplitudes  $A^{(1)} \dots A^{(5)}$ , one obtains for the QCD amplitudes at tree level

$$M_{12}^{\text{QCD}} = \frac{-g^3}{2N} (A^{(1)} + A^{(2)}) \equiv \frac{-g^3}{2N} A^{(12)} \quad (7)$$

$$M_{34}^{\text{QCD}} = \frac{-g^3}{2N} (A^{(3)} + A^{(4)}) \equiv \frac{-g^3}{2N} A^{(34)} \quad (8)$$

$$M_1^{\text{QCD}} = \frac{-g^3}{4} (A^{(1)} + A^{(2)} + A^{(3)} + A^{(4)}) \quad (9)$$

$$M_2^{\text{QCD}} = \frac{-g^3}{4} (A^{(1)} - A^{(2)} + A^{(3)} - A^{(4)} + 2A^{(5)}) \equiv \frac{-g^3}{4} A^{(\text{na})} . \quad (10)$$

The non-abelian three-gluon-vertex only contributes to the color octet exchange amplitude  $M_2$ . Both  $M_2$  and  $M_1$  vanish for  $t$ -channel photon exchange, while the color singlet exchange amplitudes are given by

$$M_{12}^{\text{QED}} = -g e_q e_Q (A^{(3)} + A^{(4)}) = -g e_q e_Q A^{(34)} \quad (11)$$

$$M_{34}^{\text{QED}} = -g e_q e_Q (A^{(1)} + A^{(2)}) = -g e_q e_Q A^{(12)} , \quad (12)$$

where  $e_q$  and  $e_Q$  denote the electric charges of the two quarks.

The resulting color and polarization summed squared amplitudes,

$$\sum |M|^2 = \frac{N^2 - 1}{2} N \sum_{\text{polarizations}} \left( |M_{12}|^2 + |M_{34}|^2 + 2 \frac{N^2 - 4}{N^2} |M_1|^2 + 2 |M_2|^2 \right) , \quad (13)$$

are shown in Fig. 2(a) for both the full QCD and the QED case and for the corresponding color singlet contributions. Shown is the dependence of  $\sum |M^2|/s$  on the rapidity of the emitted gluon when all other phase space parameters are kept fixed, namely the two quarks are held at  $p_T = 30$  GeV and pseudorapidities  $\eta_q = 3$  and  $\eta_Q = -3$  and the gluon transverse momentum is chosen to be  $p_{Tg} = 2$  GeV. The details of this choice are irrelevant: forward scattering of the two quarks is a sufficient condition to obtain the qualitative radiation pattern of Fig. 2. In the QCD case the color octet contributions, via the non-abelian amplitude  $A^{(\text{na})}$ , lead to enhanced gluon emission in the angular region between the two jets. For  $t$ -channel photon exchange this region is essentially free of gluons due to color coherence

between initial and final state gluon radiation [8,9]: gluon emission into the central region is exponentially suppressed as the rapidity distance from the quarks increases. It is exactly this difference between the QED and the QCD case which lets us expect the formation of rapidity gaps for color singlet exchange in the  $t$ -channel.

Single gluon exchange also produces a color singlet exchange piece which is defined by the  $|M_{12}|^2 + |M_{34}|^2$  term in Eq. (13). Since its shape is identical to the one for tree level photon exchange (dashed and dash-dotted lines in Fig. 2(a)), one might be misled to conclude that the color singlet contribution to single gluon exchange also produces rapidity gaps. However, there is an important difference between the two: the role of the amplitudes  $A^{(12)}$  and  $A^{(34)}$  is interchanged in the QCD *vs.* QED color singlet exchange amplitudes.

The appearance of  $A^{(12)} = A^{(1)} + A^{(2)}$  in the QED amplitude  $M_{34}^{\text{QED}}$  corresponds to the first two Feynman graphs in Fig. 1, *i.e.* emission of the final state gluon from the upper quark line. Color coherence between these two graphs strongly suppresses gluon emission except in the angular region between the initial and final direction of the upper quark  $q$  (dashed line in Fig. 2(b)). In forward quark scattering via photon exchange the color  $i_1$  of the initial quark  $q$  is thus transferred to a low mass color triplet object which emerges close to the original  $q$  direction. At lowest order this is the final state  $q$ , at  $\mathcal{O}(\alpha_s)$  it is the  $qg$  system. The situation is thus stable against gluon emission at even higher order for the QED case and gluon radiation is suppressed in the rapidity range between the two final state quarks.

Formally, the QCD amplitude  $M_{34}^{\text{QCD}}$  also describes  $t$ -channel color singlet exchange as seen from the lower quark line. Proportionality to  $A^{(34)}$  implies that the gluon is emitted from the lower quark,  $Q$ , and hence preferentially between the initial  $Q$ -beam and the final  $Q$  directions (dash-dotted line in Fig. 2(b)). Thus the color triplet  $qg$  system, into which the initial quark  $q$  evolves, consists of a widely separated quark and gluon. Higher order corrections will lead to strong gluon radiation into the angular region between the two and thus also into the rapidity range between the two final state quarks.

One thus finds that a color singlet exchange structure as identified by the color tensors is not sufficient to infer the production of a rapidity gap in the gluon radiation pattern. Stability of the pattern against multiple gluon emission is another necessary requirement. The shapes produced by  $|M_{34}^{\text{QED}}|^2$  and  $|M_{34}^{\text{QCD}}|^2$  may now be taken as a gauge for the radiation pattern produced by  $t$ -channel two-gluon exchange when the color index on the  $Q$ -quark line is preserved. Only a QED like pattern can be expected to lead to the formation of a rapidity gap in dijet events.

### III. THE IMAGINARY PART OF $M_{34}$

A complete calculation of gluon emission in  $qQ$  scattering via two-gluon exchange involves squaring box-diagrams like the ones in Fig. 3 and thus corresponds to a two-loop calculation of the 3-jet cross section at hadron colliders, which is clearly beyond the scope of the present work. Since  $qQ \rightarrow qQ$  scattering via color singlet two gluon exchange is dominated by its imaginary part at  $|t| \ll s$  [11], we restrict our attention to the imaginary part of  $M_{34}$ , as defined by unitarity,

$$\begin{aligned}
2(\text{Im} T)_{fi} &\equiv \frac{1}{i}(T_{fi} - T_{fi}^\dagger) \\
&= \int \prod_{j=1}^n \frac{d^3 p_j}{(2\pi)^3 2p_j^0} (2\pi)^4 \delta^4(\sum_{j=1}^n p_j - p_i) T_{fn}^\dagger T_{ni}.
\end{aligned} \tag{14}$$

Here  $n$  denotes the number of on-shell intermediate particles and  $i = |qQ\rangle$  and  $f = |qQg\rangle$  symbolize the initial and final state.

To lowest order,  $\mathcal{O}(g^5)$ , only  $n = 2$  and  $n = 3$  particle intermediate states contribute to  $\text{Im}(M_{34})$ . Representative Feynman graphs are depicted in Fig. 3. Row a) shows graphs corresponding to  $n = 2$  particle intermediate states  $|qQ\rangle$ . Factoring out color factors and coupling constants, the contributions to  $T_{fn}^\dagger T_{ni}$  are given by the products of the tree level amplitudes listed below the individual Feynman diagrams. Here  $B_i$  corresponds to the 1-gluon exchange graph in  $qQ$  elastic scattering and the  $A_f^{(j)}$  are the tree level  $qQ \rightarrow qQg$  amplitudes of Fig. 1. When considering  $qQg$  3-particle intermediate states at order  $g^5$  the  $3 \rightarrow 3$  amplitude decomposes into one disconnected particle and a tree level  $2 \rightarrow 2$  amplitude. The three possibilities are shown in rows b), (disconnected gluon), c) (disconnected quark  $Q$ ), and d) (disconnected quark  $q$ ) of Fig. 3.  $B_f$  refers to the tree level  $qQ \rightarrow qQ$  1-gluon exchange graph and  $C_f^{(j)}$  and  $D_f^{(j)}$  ( $j = 1, 2, 3$ ) correspond to the three tree level graphs contributing to  $qg \rightarrow qg$  and  $Qg \rightarrow Qg$  scattering, respectively.

Because of the disconnected particle in the  $3 \rightarrow 3$  amplitudes the phase space integral in the unitarity relation of Eq. (14) reduces to a solid angle integral over the direction of one of the two intermediate state particles participating in the scattering, taken in the two particle rest frame. Using the abbreviations  $A^{(12)}$ ,  $A^{(34)}$ , and  $A^{(na)}$  (see Eq. (7)–(10)) for the gauge invariant combinations of tree level  $qQ \rightarrow qQg$  amplitudes, one finds

$$\begin{aligned}
\text{Im}(M_{34}) &= \frac{g^5}{16N^2 32\pi^2} \int d\Omega \left( -B_i \left[ -N^2 A_f^{(na)} + (N^2 - 2)A_f^{(12)} + (N^2 - 4)A_f^{(34)} \right] \right. \\
&\quad - \left[ N^2 A_i^{(na)} + (N^2 - 2)A_i^{(12)} + (N^2 - 4)A_i^{(34)} \right] B_f \\
&\quad + 2A_i^{(34)} \left[ (N^2 - 1)C_f^{(1)} - C_f^{(2)} + N^2 C_f^{(3)} \right] \\
&\quad + \left[ (N^2 - 4)A_i^{(12)} + (N^2 - 2)A_i^{(34)} \right] \left[ D_f^{(1)} + D_f^{(2)} \right] \\
&\quad \left. + N^2 A_i^{(na)} \left[ D_f^{(1)} - D_f^{(2)} + 2D_f^{(3)} \right] \right).
\end{aligned} \tag{15}$$

Because of the massless  $t$ -channel gluon propagators in the Feynman graphs of Fig. 1 the phase space integral in Eq. (15) actually diverges. The same problem is already encountered for Low-Nussinov Pomeron exchange in  $qQ$  elastic scattering and can be circumvented by replacing the massless gluon propagator by a regularized version which avoids gluon propagation over long distances [4]. QCD Pomeron models of this kind, with a dynamically generated gluon mass [12], have been found to give a good description of available data [13]. We approximate these refinements by multiplying the four products  $T_{fn}^\dagger T_{ni}$  in the unitarity relation (corresponding to the four groups of intermediate states in Fig. 3) by factors

$$\frac{q^2}{q^2 - m_r^2}, \quad m_r = 300 \text{ MeV} \tag{16}$$

for each internal gluon propagator of momentum  $q$ . Effectively this corresponds to a replacement of a massless propagator by a massive one. Since any complete gauge invariant set of amplitudes is multiplied by a common factor, gauge invariance is preserved by this procedure. Finally, the phase space integral of Eq. (15) was performed numerically by evaluating individual tree level amplitudes with the aid of the helicity amplitude techniques of Ref. [14]. The numerical evaluation of this “loop”-integral is quite slow (of order ten minutes for one individual phase space point on our Alpha-station) and does not allow detailed investigations via a Monte Carlo program. However, the code is quite adequate for a first qualitative study.

#### IV. RADIATION PATTERN FOR TWO-GLUON EXCHANGE

Numerical results for  $|M_{34}|^2/s$  are shown in Fig. 4. The square of this color singlet exchange amplitude was obtained for particular kinematic configurations (the same ones as used in Section II) where the two quarks are held fixed at  $p_T = 30$  GeV and pseudorapidities  $\eta_q = 3$  and  $\eta_Q = -3$  as indicated by the arrows. The gluon then is taken at fixed  $p_{Tg} = 2(15)$  GeV and the gluon rapidity is varied between -8 and +8. The solid lines depict the gluon angular distribution for the imaginary part of the two gluon exchange amplitude,  $Im(M_{34})$ . The distributions follow neither the ones for  $t$ -channel photon exchange (dashed lines) nor the ones for color octet single gluon exchange (dash-dotted lines). Rather one finds a strong enhancement in the central region,  $-3 < \eta_g < 3$ , which is particularly pronounced for the emission of high transverse momentum gluons.

This enhancement can be traced to Feynman graphs like the first one in Fig. 5, the  $A_i^{(5)} D_f^{(3)}$  term. Since the upper quark,  $q$ , is fixed at small scattering angle, this diagram corresponds to  $q \rightarrow g$  splitting and subsequent elastic  $gQ$  scattering by  $t$ -channel color singlet two gluon exchange, *i.e.* by the exchange of a Low-Nussinov Pomeron. There is no reason why this process should be suppressed except for  $\eta_g < \eta_Q$ , which corresponds to large scattering angles in the  $gQ$  rest frame. Indeed the fall-off observed in Fig. 4 at  $\eta_g < -3$  confirms this interpretation.

In order to isolate gluon radiation off “Pomeron exchange” between the two quark lines one needs to eliminate the collinear contributions involving Pomeron exchange between the gluon and the quarks. A full treatment of the collinear region requires convolution with quark and gluon structure functions. Because we do not yet have analytic formulas for the imaginary part or at least a fast Monte Carlo program, we cannot at present perform the full calculation. However, for our qualitative discussion a crude approximation will suffice. From the full amplitude  $Im(M_{34})$  we subtract the gluon box diagram  $A_i^{(5)} D_f^{(3)}$  of Fig. 5 and the minimal set of additional graphs required for gauge invariance. We thus define the Pomeron amplitude in  $qQ \rightarrow qQg$  scattering as

$$Im(M_{34}^{\text{Pom}}) = Im(M_{34}) - \frac{g^5}{16N^2} \frac{1}{32\pi^2} \int d\Omega \left( 4N^2 [A_i^{(5)} + A_i^{(3)} - A_i^{(2)}] [D_f^{(1)} + D_f^{(3)}] \right). \quad (17)$$

The above choice is fixed not by gauge invariance alone, but rather by the necessity to avoid over-subtraction in all regions of phase space. While the combination  $-D_f^{(2)} + D_f^{(3)}$  for the last factor in Eq. (17) is gauge invariant also, the concomitant contribution  $A_i^{(5)} D_f^{(2)}$  (see second graph in Fig. 5) is strongly peaked for back-scattered gluons and thus would not

correspond to Pomeron exchange in  $gQ$  scattering. Similarly, the  $s$ -channel quark exchange graphs  $A_i^{(2)}$  and  $A_i^{(3)}$  (see Fig. 1) are chosen to form a gauge invariant combination with  $A_i^{(5)}$ . The additional pieces are numerically small, unlike  $A_i^{(1)}$  and  $A_i^{(4)}$  terms which receive strong enhancements from the  $u$ -channel quark propagators and lead to over-subtraction in the  $\eta_g > \eta_q$  and  $\eta_g < \eta_q$  regions, respectively.

The resulting radiation pattern in “Pomeron exchange” between the two quark lines is given in Fig. 6 for three values of the regularizing gluon mass parameter,  $m_r = 0.3$  GeV (solid lines),  $m_r = 0.15$  GeV (dotted lines), and  $m_r = 1$  GeV (dash-double dotted lines). The  $p_{Tg} = 2$  GeV case shows that soft gluon emission strongly resembles the pattern found for  $t$ -channel photon exchange: emission into the gap region between the two quarks and backwards emission are strongly suppressed. Soft gluon radiation in Pomeron exchange therefore produces the pattern expected for  $t$ -channel color singlet exchange, and as argued earlier for photon exchange this pattern should be preserved for multiple soft gluon emission. This strongly suggests that quark scattering by exchange of a hard Pomeron indeed leads to the formation of rapidity gaps in dijet events [6,10]. For hard gluon radiation ( $p_{Tg} = 15$  GeV in Fig. 6(b)) backward emission, like in the QCD case, dominates and no suppressed radiation into the gap region can be expected at higher orders.

Qualitatively, the radiation pattern in Pomeron exchange,  $Im(M_{34}^{\text{Pom}})$ , can be described as a superposition of a QED-like component, which dominates at small gluon transverse momenta, and a QCD-like component, which dominates in the hard region. The transition between the soft and hard regions is displayed in Fig. 7 by showing  $|M_{34}|^2/s$  as a function of  $p_{Tg}$  for the same quark configuration as in Fig. 6. In the back-scattering region (see Fig. 7(a)) the emission of soft gluons is severely suppressed compared to the tree level QCD case. In the forward region (see Fig. 7(b)) soft gluon emission in “Pomeron exchange” essentially follows the shape expected for photon exchange. For large gluon transverse momenta, however, the QED-like component of  $Im(M_{34}^{\text{Pom}})$  is severely suppressed.

The more QCD-like behavior at large  $p_{Tg}$  may be understood by noting that the phase space integral for color singlet two-gluon exchange in Eq. (15) is dominated by the region of small  $|q^2|$  for one of the two gluons. A hard radiated gluon is insensitive to the color screening by this soft gluon and effectively only the color charge of the second, hard  $t$ -channel gluon is seen, leading to a more QCD-like radiation pattern.

This interpretation is confirmed in Figs. 6 and 7 by the curves for different values of the regularizing gluon mass. Larger values of  $m_r$  eliminate the soft gluon exchange region where the emitted gluon can resolve the color charges of the two  $t$ -channel gluons. Thus the color singlet structure of  $t$ -channel two gluon exchange gains importance and the radiation pattern becomes more QED-like.

Figs. 6 and 7 also exhibit the dependence of our results on the regularization of the gluon propagator. In the regions of strong destructive interference in  $Im(M_{34})$ , which are visible in Fig. 6, the quantitative results strongly depend on the details of soft gluon exchange and are thus non-perturbative in nature. The qualitative features, however, suppression of backwards soft gluon emission in color singlet two gluon exchange events and a more QCD-like behavior in the hard region, are insensitive to these uncertainties. In particular, the variation with  $m_r$  is modest in the most important region, forward gluon emission at small  $p_{Tg}$ . Hence, our main finding, the QED like radiation pattern of soft gluons in Pomeron exchange, is unaffected.



## V. CONCLUSIONS

We have analyzed the different properties of  $t$ -channel color singlet *vs.* color octet exchange processes in  $qQ$  scattering at next to leading order, namely including gluon bremsstrahlung. The radiation pattern of emitted gluons is intimately connected, after hadronization, to the angular distribution of produced hadrons and hence directly bears on the question whether rapidity gaps are to be expected in  $t$ -channel color singlet exchange processes. Essentially, we arrive at an affirmative answer, also for the case of color singlet two gluon exchange.

While this answer was expected by many in the field, our calculations reveal a rich internal structure of the Pomeron. In addition, our demonstration had to deal with a number of problems which do not yet appear at the level of  $2 \rightarrow 2$  processes. While the definition of  $t$ -channel color singlet exchange is obvious in the case of  $qQ \rightarrow qQ$  scattering, the emission of an extra gluon complicates the picture. The color tensors of the  $qQ \rightarrow qQg$  process suggest identification of color singlet exchange as those terms where the color of at least one of the incident quarks remains unchanged. In the QCD case (single gluon exchange) this also occurs since the color of the exchanged gluon can be compensated for by emission of a gluon of the same color. The crucial difference emerges when considering the angular distribution of emitted gluons:  $t$ -channel photon exchange leads to forward gluon emission and hence preserves the spatial distribution of the color charges which are present at lowest order. By contrast gluons are radiated in the backwards direction in the QCD color singlet term, and multiple emission will wash out the pattern produced by the first emitted gluon.

Color singlet and color octet exchange terms do not interfere because they are orthogonal in color. Because of their different behaviour under multiple gluon emission any interference between a QED- and a QCD-like “color singlet pattern” will be severely suppressed at higher order. The square of the QED-like component in the color singlet exchange amplitude can hence be treated as the probability density for producing a hard scattering event which may evolve into a rapidity gap signature. For technical reasons (numerical speed) we cannot yet calculate rapidity gap cross sections, rather we are limited to an analysis at the amplitude square level when considering the  $t$ -channel exchange of two gluons.

For  $t$ -channel two gluon exchange we have calculated the imaginary part of the color singlet exchange amplitude,  $Im(M_{34})$ , and we have analyzed the emission probability for the extra gluon when the quarks are scattered by small angles only. At first sight gluon emission is most likely in the angular region between the two quarks. However, this pattern is solely due to  $q \rightarrow g$  splitting and subsequent  $gQ$  scattering via the exchange of a Low-Nussinov Pomeron. Only after subtracting this contribution does the final pattern emerge for gluon emission in  $qQ$  scattering via Pomeron exchange.

For high transverse momentum of the emitted gluon (of order of the quark momenta) the radiation pattern is quite similar to the one obtained for single gluon exchange. Hard emitted gluons have too short a wavelength to see the screening of the color charge of the harder exchanged gluon by the second, typically very soft, exchanged gluon. The Low-Nussinov Pomeron thus reveals itself as an extended object. Hard gluon emission is able to resolve the internal color structure of the Pomeron.

As the transverse momentum of the emitted gluon is decreased, a qualitative transition occurs. The gluon radiation can no longer resolve this internal color structure and hence the

Pomeron appears as a color singlet object. As a result the emission of a soft gluon ( $p_{Tg} \ll p_{Tq}$ ) follows a pattern very similar to the one observed for  $t$ -channel photon exchange. This pattern is expected to lead to the formation of rapidity gaps. Since the overall gluon emission rate is dominated by the soft region, we conclude that two gluon color singlet exchange in dijet events may indeed lead to the formation of rapidity gap events as observed at the Tevatron [5].

**Acknowledgements** We thank J. D. Bjorken, S. Ellis, F. Halzen, and G. Sterman for helpful discussions. This research was supported in part by the University of Wisconsin Research Committee with funds granted by the Wisconsin Alumni Research Foundation, by the U. S. Department of Energy under contract No. DE-AC02-76ER00881, and by the Texas National Research Laboratory Commission under Grants No. RGFY9273 and FCFY9212.

## REFERENCES

- [1] See *e.g.* L. V. Gribov, E. M. Levin, and M. G. Ryskin, *Phys. Rep.* **100C** (1983) 1; E. M. Levin and M. G. Ryskin, *Phys. Rep.* **189C** (1990) 267, and references therein.
- [2] F. E. Low, *Phys. Rev.* **D12** (1975) 163; S. Nussinov, *Phys. Rev. Lett.* **34** (1975) 1286.
- [3] Ya. Ya. Balitsky and L. N. Lipatov, *Sov. J. Nucl. Phys.* **28** (1978) 822.
- [4] P. V. Landshoff and O. Nachtmann, *Z. Phys.* **C35** (1987) 405.
- [5] D0 Collaboration, S. Abachi et al., *Phys. Rev. Lett.* **72** (1994) 2332.
- [6] J. D. Bjorken, *Int. J. Mod. Phys.* **A7** (1992) 4189; *Phys. Rev.* **D47** (1993) 101; preprint SLAC-PUB-5823 (1992).
- [7] E. Gotsman, E. M. Levin, and U. Maor, *Phys. Lett.* **B309** (1993) 199.
- [8] Y. L. Dokshitzer *et al.*, *Rev. Mod. Phys.* **60** (1988) 373, and references therein.
- [9] R. S. Fletcher and T. Stelzer, *Phys. Rev.* **D48** (1993) 5162.
- [10] H. Chehime *et al.*, *Phys. Lett.* **B286** (1992) 397.
- [11] J. R. Cudell and B. U. Nguyen, preprint McGill 93-25 (1993).
- [12] J. M. Cornwall, *Nucl. Phys.* **B157** (1979) 392; *Phys. Rev.* **D26** (1982) 1453.
- [13] F. Halzen, G. I. Krein, and A. A. Natale, *Phys. Rev.* **D47** (1992) 295; M. B. Gay Ducati, F. Halzen, and A. A. Natale, *Phys. Rev.* **D48** (1993) 2324.
- [14] K. Hagiwara and D. Zeppenfeld, *Nucl. Phys.* **B274** (1986) 1; *ibid.* **B313** (1989) 560.

## FIGURES

FIG. 1. Feynman graphs for the process  $qQ \rightarrow qQg$  via  $t$ -channel gluon exchange.

FIG. 2. Rapidity distribution of emitted gluons in  $uc \rightarrow ucg$  scattering. The final state quarks are kept fixed at forward rapidities of  $\eta_q = \pm 3$  (indicated by the arrows) and transverse momenta  $p_{Tq} = 30$  GeV while the gluon rapidity is varied between -8 and 8 at fixed transverse momentum  $p_{Tg} = 2$  GeV. In part a) results are shown for the sum over all color structures for single gluon exchange (dash-double-dotted line) and for  $t$ -channel photon exchange (dashed line). In addition the QCD color singlet exchange contribution, as defined by the  $M_{12}$  and  $M_{34}$  terms in Eq. (13), is shown (dash-dotted line). The  $M_{34}$  terms alone, in part b), demonstrate the difference between the QED and the QCD color singlet exchange terms.

FIG. 3. Feynman graphs contributing to the imaginary part of the  $qQ \rightarrow qQg$  amplitude at order  $g_s^5$ . The four groups correspond to  $qQ$  intermediate states (a) and three parton intermediate states with subsequent  $qQ$  scattering (b),  $qg$  scattering (c), and  $Qg$  scattering (d). The dashed vertical line shows where to make the cut in order to obtain the imaginary part. The corresponding product of tree level  $2 \rightarrow 2$  and  $2 \rightarrow 3$  amplitudes is given below each graph. The crosses on the propagators of the  $2 \rightarrow 3$  tree level sub-amplitudes indicate the other positions where the external gluon propagator needs to be attached.

FIG. 4. Rapidity distribution of emitted gluons in  $uc \rightarrow ucg$  scattering. Results are shown for the color singlet contribution as seen by the charm quark ( $12|M_{34}|^2/s$ ). The final state quarks are kept fixed at forward rapidities of  $\eta_q = \pm 3$  and transverse momenta  $p_{Tq} = 30$  GeV while the gluon rapidity is varied between -8 and 8. Results are shown for the case of a) a “soft” gluon of  $p_{Tg} = 2$  GeV and b) a hard gluon of  $p_{Tg} = 15$  GeV. The solid lines give the results for the full imaginary part of the color singlet exchange amplitude  $M_{34}$ . For comparison the tree level results for  $12|M_{34}|^2/s$  are shown for gluon exchange (dash-dotted lines) and photon exchange (dashed lines).

FIG. 5. Two of the Feynman graphs corresponding to  $q \rightarrow g$  splitting and subsequent  $gQ$  scattering.

FIG. 6. Rapidity distribution of emitted gluons in  $uc \rightarrow ucg$  scattering. Results are shown for the color singlet contribution as seen by the charm quark ( $12|M_{34}|^2/s$ ) after subtraction of the “Pomeron” contribution to  $u \rightarrow g$  splitting and subsequent  $cg$  scattering (see text). The dotted, solid, and dash-double-dotted lines show the gluon radiation pattern for three different values of the regularizing gluon mass,  $m_r$ . The phase space configurations are the same as in Fig. 4. For comparison tree level results for  $12|M_{34}|^2/s$  are shown for gluon exchange (dash-dotted lines) and photon exchange (dashed lines).

FIG. 7. Dependence of the color singlet exchange amplitude,  $12|M_{34}|^2/s$ , on the gluon transverse momentum  $p_{Tg}$  at two values of the gluon scattering angle, a)  $\eta_g = -5$  and b)  $\eta_g = +5$ . The final state quarks are fixed at the same momenta as in Fig. 4. Results are shown for three values of the regularizing gluon mass,  $m_r = 0.15$  GeV (dotted line),  $m_r = 0.3$  GeV (solid line), and  $m_r = 1$  GeV (dash-double-dotted line). For comparison, the corresponding QCD and QED distributions are also shown.

This figure "fig1-1.png" is available in "png" format from:

<http://arxiv.org/ps/hep-ph/9401244v2>

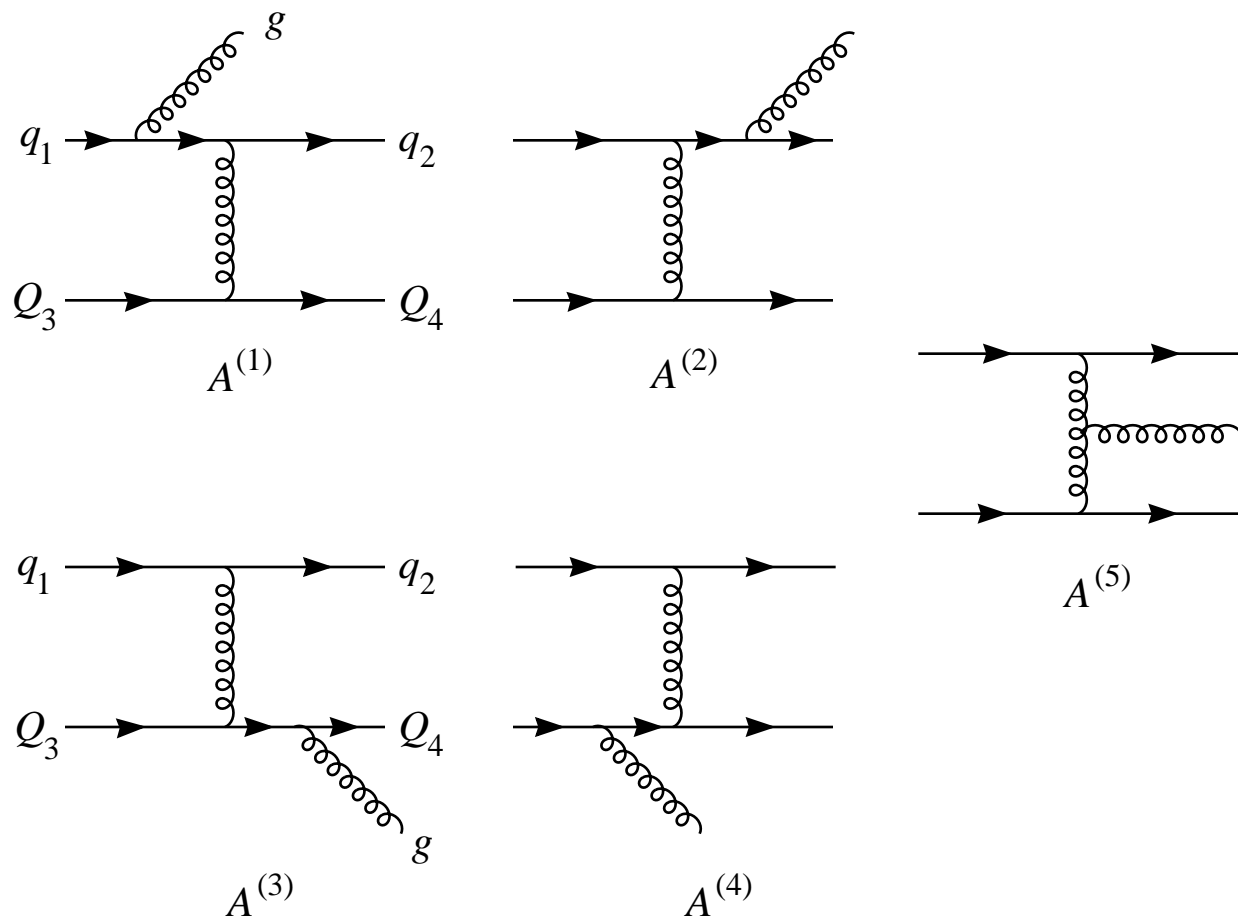


Fig. 1



This figure "fig2-1.png" is available in "png" format from:

<http://arxiv.org/ps/hep-ph/9401244v2>

This figure "fig3-1.png" is available in "png" format from:

<http://arxiv.org/ps/hep-ph/9401244v2>

This figure "fig4-1.png" is available in "png" format from:

<http://arxiv.org/ps/hep-ph/9401244v2>

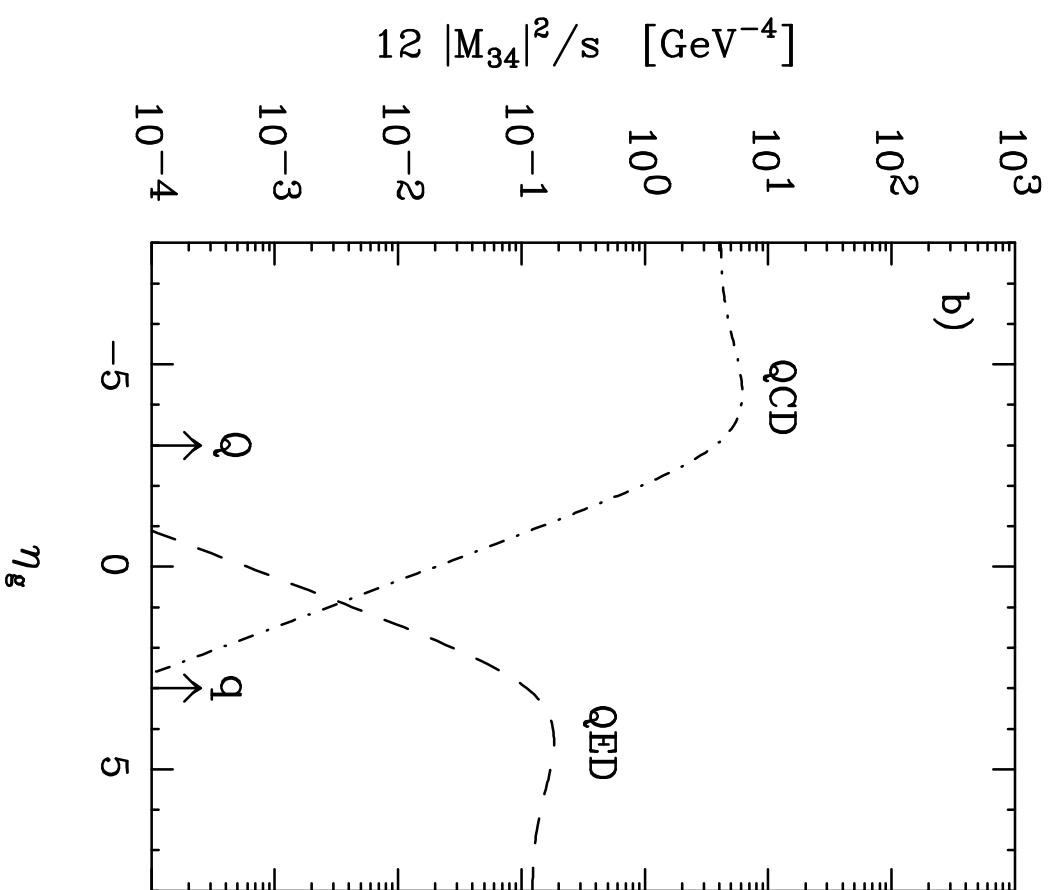
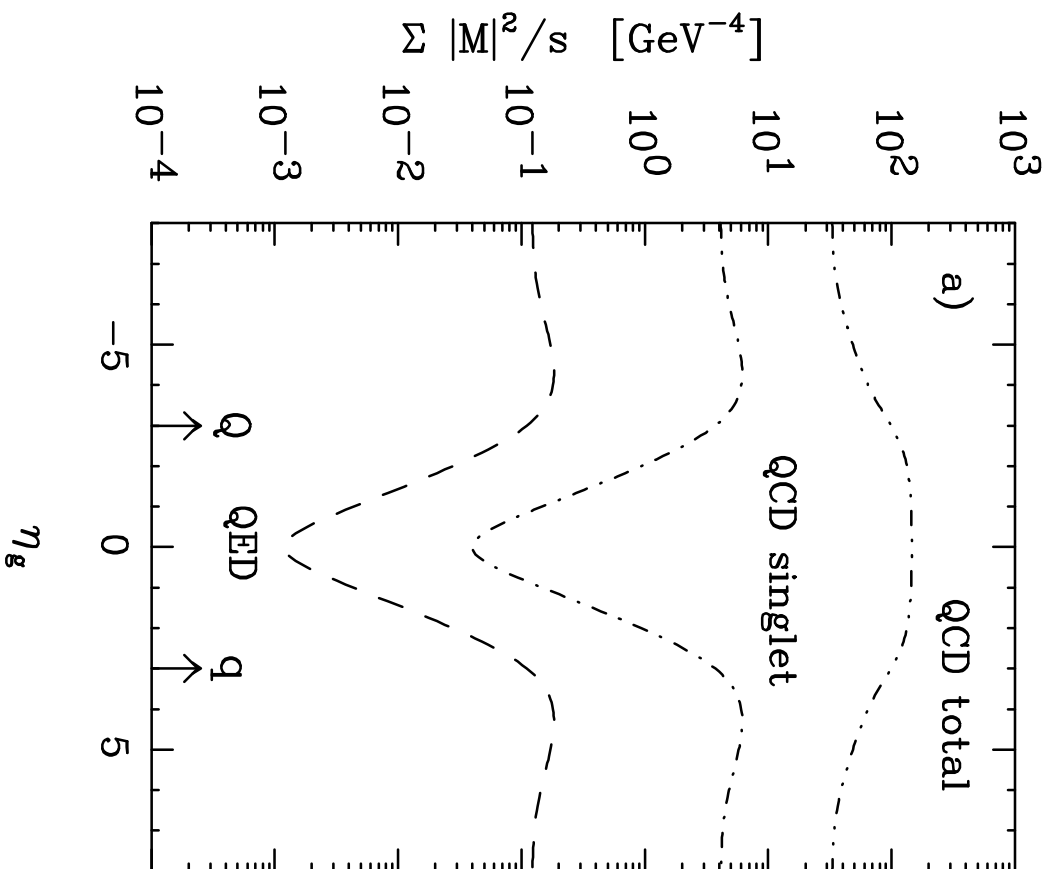


Fig. 2

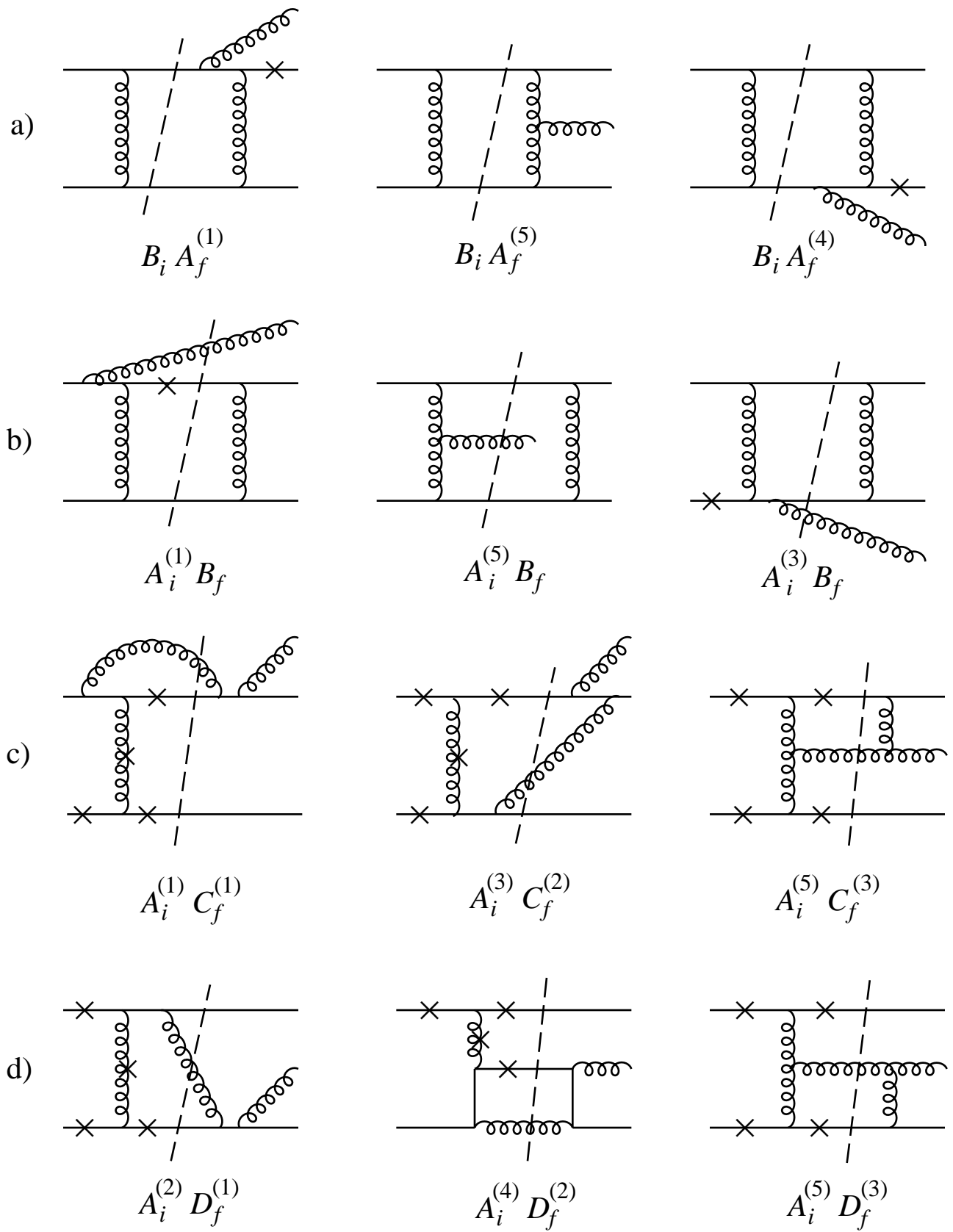


Fig. 3

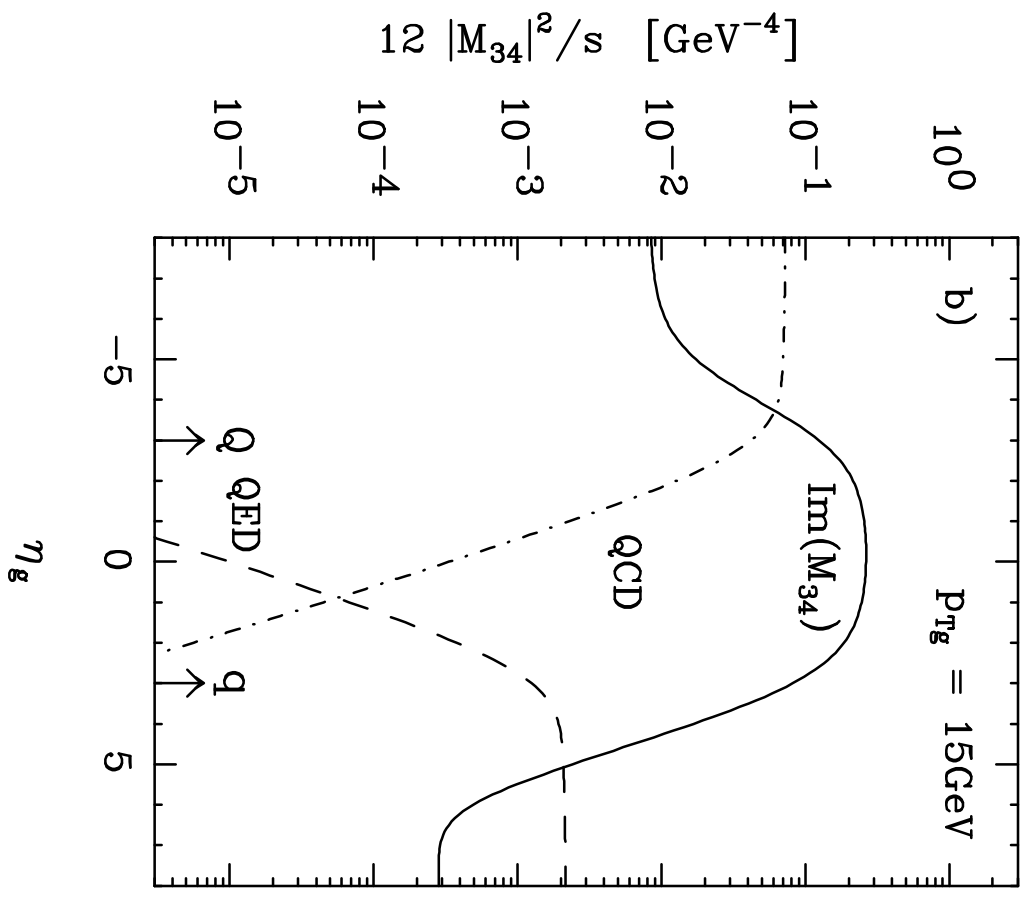
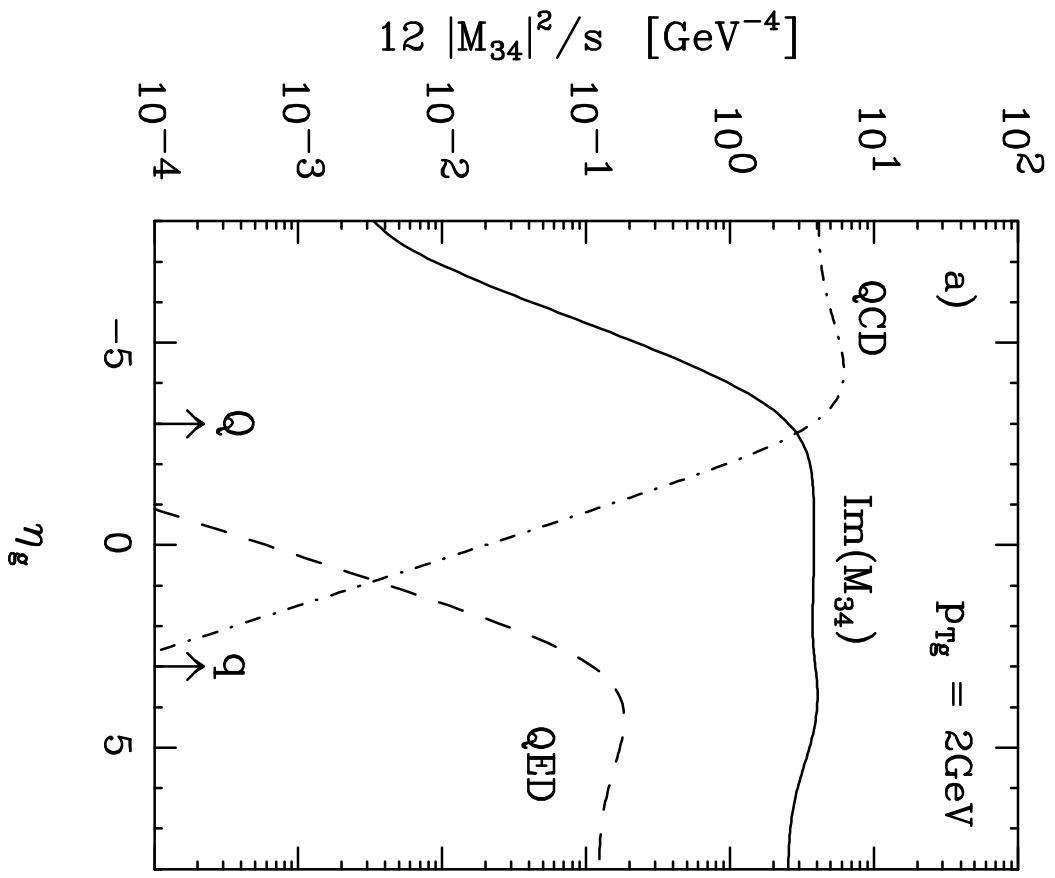
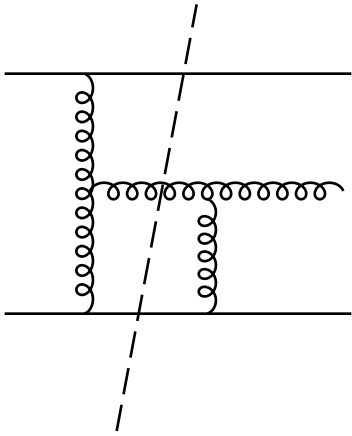
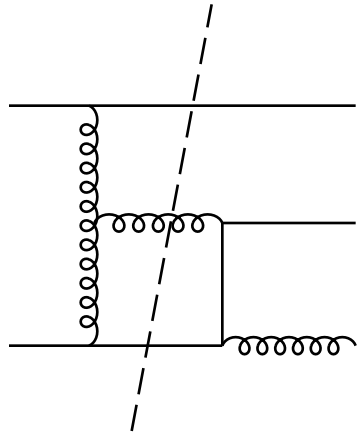


Fig. 4



$$A_i^{(5)} D_f^{(3)}$$



$$A_i^{(5)} D_f^{(2)}$$

Fig. 5

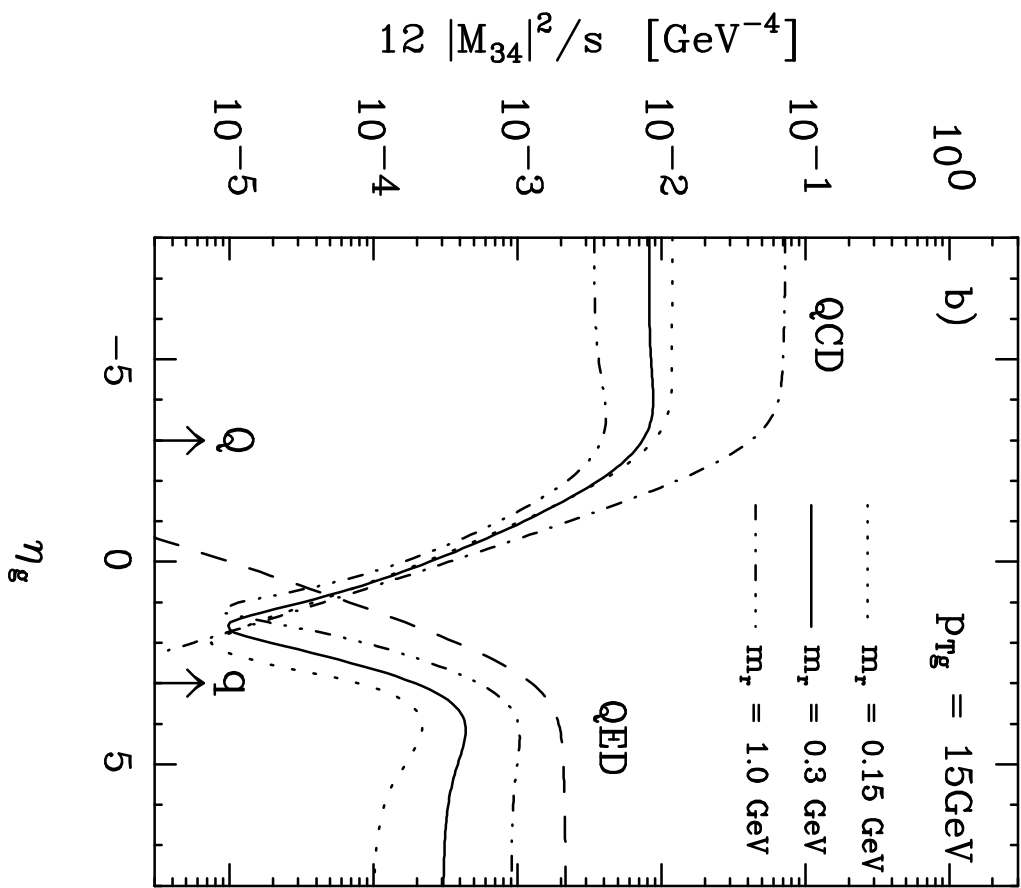
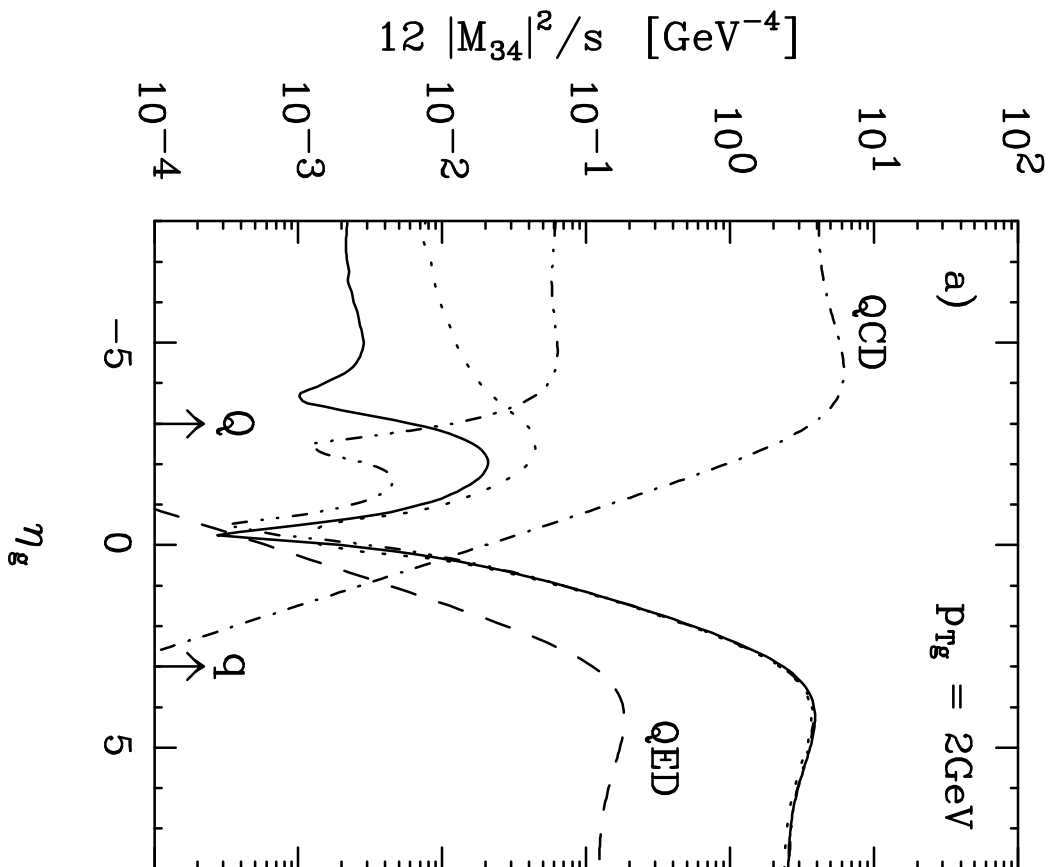


Fig. 6



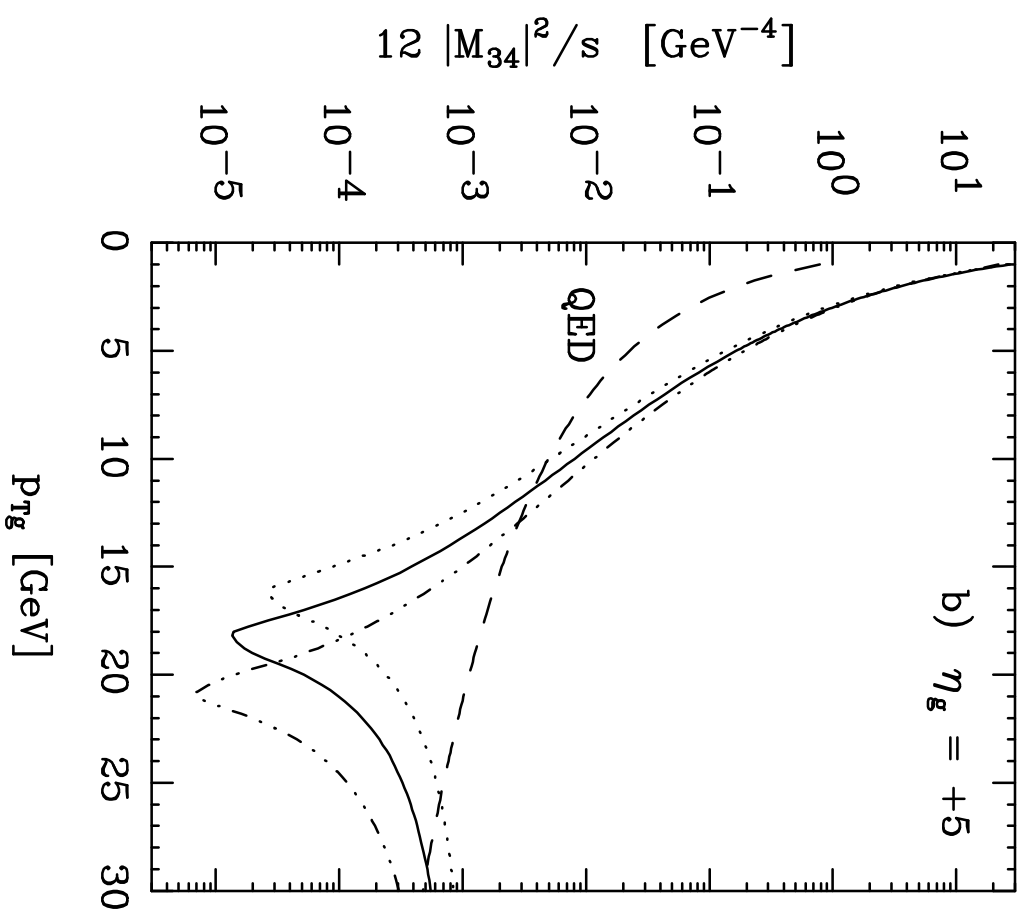
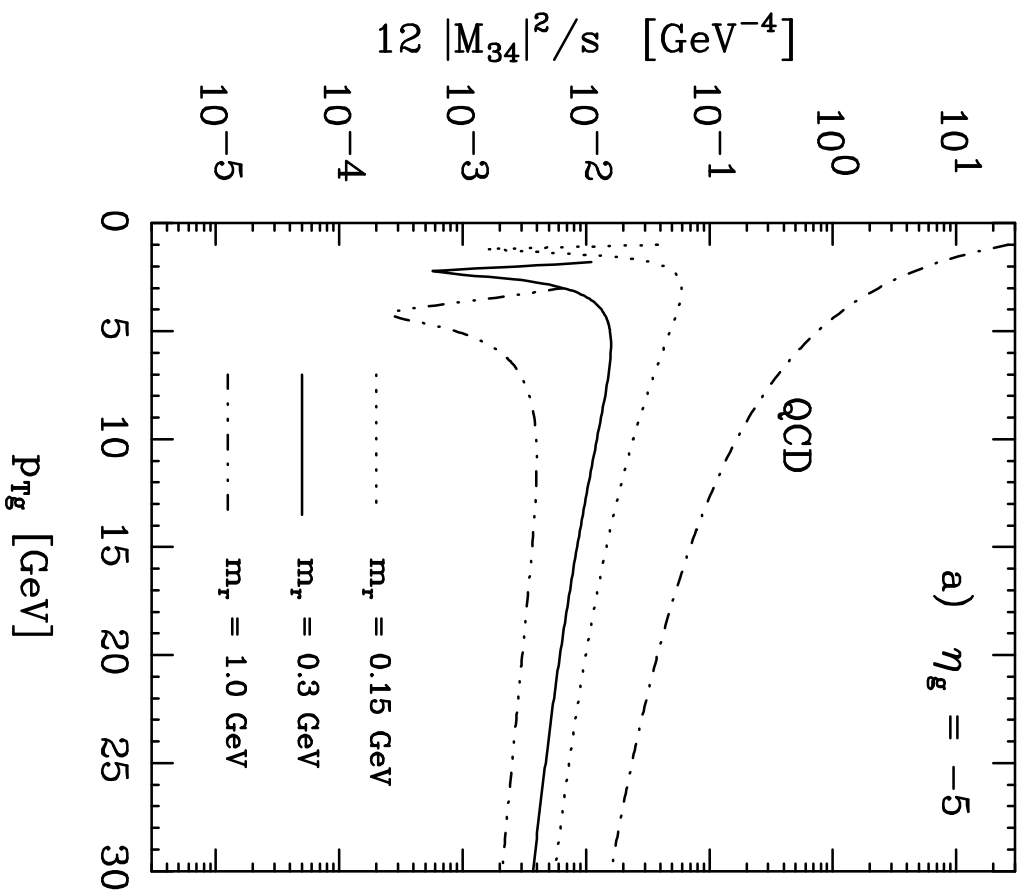


Fig. 7